Journal of Catalysis **201,** 105–112 (2001)
doi:10.1006/jcat.2001.3240, available online at http://www.idealibrary.com on IDEAL®

Iron-Containing Graphite as a Friedel-Crafts Alkylation Catalyst

Masatoshi Nagai,*[,1] Takeshi Yoda, Shinzo Omi,* and Mistuo Kodomari†

*Graduate School of Bio-applications and Systems Engineering, Tokyo University of Agriculture and Technology, 2-24 Nakamachi, Koganei, Tokyo 184-8588, Japan; and †Department of Industrial Chemistry, Shibaura Technological University, 3-9 Shibaura, Minato, Tokyo 108-8548, Japan

Received January 15, 2001; revised March 29, 2001; accepted March 29, 2001; published online May 31, 2001

The activity of iron-containing graphites for the Friedel-Crafts reaction of phenol with *tert*-butyl halides was studied. Graphites were characterized by XRD and XPS. The reaction of phenol with either various *tert*-butyl halides or *tert*-butyl alcohol on iron-containing graphite was performed in a benzene solvent for 4 h at 50°C. The conversion and yield of the reaction on iron-containing graphite decreased in the order, *tert*-butyl iodide, *tert*-butyl bromide, and *tert*-butyl chloride, whereas for $AlCl_3$, *tert*-butyl chloride was the most reactive while *tert*-butyl iodide was the least. Activated charcoal was not reactive. The presence of iron accelerated the reaction of phenol with the *tert*-butyl halide on graphite to yield *p-tert*-butylphenol as the main product. The presence of both *tert*-butyl bromide and iron increased the distance between the layers of graphite but not in the presence of either the iron or *tert*-butyl bromide. *tert*-Butyl halide was first adsorbed on graphite and then dissociated to form *tert*-butyl and halogen ions. The peak was observed at $d = 11.9$ Å in the XRD pattern of the graphite after the reaction in which the high purity graphite was treated with *tert*-butyl halide and iron in phenol. This is probably due to the mixture of phenol with *tert*-butyl ion and iron inserted into the layers of graphite to form a two-stage structure.

INTRODUCTION

The Friedel-Crafts reaction is known to be an important method of introducing alkyl and acyl groups into aromatic compounds. Aluminum chloride, in general, is the most widely used catalyst for this reaction, but it is not easily recovered. Wastes containing aluminum chloride stain the equipment and are discharged to produce a large amount of toxic acidic fluids. Acid solids have been proposed as suitable catalysts for resolving these problems. Zeolites (1, 2), ZSM-5 (3, 4), mesoporous silica (5), and alumina (6) catalyzed the shape-selective alkylation of benzene, phenol, and naphthalene with formaldehyde and *tert*-butyl and benzyl compounds. Furthermore, the acylation of anisole, benzene, and *p*-xylene over heteropolyacids (7), sulfated zirconia catalysts (8), Nafion/silica (9), and ZSM-5 (10, 11) were reported as a Brønsted catalyst instead of $AlCl_3$. In the case of clays, Fe- and Zn-modified montmorillonite (12–14) and smectites (15) catalyzed the Friedel-Crafts alkylation. On the other hand, graphite behaves like a Lewis acid and is characteristic of a layered structure. Intercalation compounds with many compounds in the layers are used to obtain special properties. Graphite can be easily recovered by simple filtration after the reaction and is reused without loss of activity. Also, the process available with the graphite does not produce waste acid liquids. Although graphite intercalation compounds have been studied extensively (16–26), few studies have been reported concerning utilization as catalysts: graphites (27, 28) and $FeCl_3$- and $AlCl_3$-graphites (29, 30) were reported to catalyze the Friedel-Crafts as a Lewis acid. Graphite-sulfuric acid (31) was reported to be active for the isomerization of trimethylbenzenes and graphite-potassium and lithium in THF for anionic polymerization of lactones (32). In this study, the purpose of the present paper is to facilitate the alkylation of phenol with *tert*-butyl bromide on iron-containing graphite, to determine the promoting effect of iron on the reaction, and to compare it with the reaction in the presence of $AlCl_3$. The relationship among the surface and bulk properties of iron-containing graphite and the catalytic activity and selectivity of three kinds of *tert*-butyl halides (Cl, Br, and I) and the stage structure of the iron-containing graphite with *tert*-butyl bromide in the reaction were studied. The mechanism for the Friedel-Crafts reaction of phenol with *tert*-butyl bromide on the iron-containing graphite was also examined.

EXPERIMENTAL

Catalysts and Reagents

Phenol, *o-tert*-butylphenol, benzene (Kishida Chemical, specific grade), Fe_2O_3, and $FeCl_3$ (specific grade) were used without purification. Synthetic graphite (Aldrich) (ALG), produced from petroleum pitch and tars, was mainly used. The other graphites also used for comparison included synthetic graphite (Kishida Chemical; C, 99.9%; Fe, 300 ppm; other metals, 5 ppm) (KIG), mineral graphite (Kishida Chemical, 78%), high purity graphite (Tokai Carbon Co; C,

[1] To whom correspondence should be addressed. Fax: +81-42-3887060. E-mail: mnagai@cc.tuat.ac.jp.

0021-9517/01 $35.00

99.99%) (HPG), activated charcoal (Merck), and fullerene (Matsubo, a mixture of C_{60} and C_{70}). Aluminum chloride, the *tert*-butyl halides (chloride, bromide, and iodine), and *tert*-butyl alcohol (Kishida Chemical) were also used without purification.

Equipment and Procedure

The reaction was carried out in a 50-ml round-bottom flask in a water bath, provided with a magnetic stirrer, a thermocouple, and a reflux condenser connected to a 10% aqueous solution of sodium hydrate to absorb acidic gas formed during the reaction. The temperature in the water bath was controlled by a thermocouple at 50°C. For each conventional reaction, 8 mmol of phenol and *tert*-butyl bromide and 4 g of graphite in 20 ml of benzene were simultaneously mixed and stirred at 50°C for 4 h. The reaction was monitored using a syringe (0.1 ml) every 30 min by gas chromatography. In order to study the preferential adsorption of *tert*-butyl bromide on iron-containing graphite, the following two reaction procedures were used: (Method A) The flask was charged with ALG, *tert*-butyl bromide, and benzene and then stirred at 50°C for 1 h before the phenol was added. (Method B) The flask was charged with ALG, phenol, and benzene and then stirred at 50°C for 1 h before the *tert*-butyl bromide was added. Furthermore, *tert*-butyl halide (bromide, chloride, or iodine) (2 mmol) was added to the mixture of phenol (5 ml) with ALG at 20°C for 1 h. For the reaction with $AlCl_3$ instead of ALG, the reaction products were extracted with diethyl ether after the reaction. For the promoting effect of iron on the reaction, Fe_2O_3 (0.004, 0.008, and 0.016 g) and $FeCl_3$ (0.008 g) were added to the mixture solution. The reaction products were analyzed using a Shimadzu GC-14B gas chromatograph equipped with flame ionization using an HR-1 capillary column. *o-tert*-Butylphenol, *p-tert*-butylphenol, bromophenol, and 2,4-di-*tert*-butylphenol were quantitatively analyzed using calibration curves. For the reaction with $AlCl_3$, the analysis was done using an internal standard method (naphthalene) after extraction of the reaction mixture with diethyl ether. The reaction products were also identified with a Hewlett-Packard 5890 gas chromatograph coupled to a Jeol Automass System III mass spectrometer. The GC was equipped with a 2 m × 0.53 mm deactivated fused-silica precolumn and a 30 m × 0.32 mm J&W DB-1 capillary column. Conversion (%) is given as the conversion of the feed (phenol or *o-tert*-butylphenol) into the products (*o*- and *p-tert*-butylphenols).

Characterization of Graphite

Crystallographic identification of the graphites was performed using powder X-ray diffraction with Ni-filtered Cu$K\alpha$ radiation (XRD, a Rigaku X-ray diffractometer (RAD-IIC)). The X-ray diffraction was collected at 30 kV and 20 mA ($\lambda = 1.5418$ Å) with a scanning speed of 2° (2θ) min^{-1} from 5 to 120°. The peaks in the spectra were identified using JPCD cards. The XRD measurements were performed in order to determine the stage structure of the graphites after the reaction with the halides, the wetted graphite, and the HPG treated with *tert*-butyl bromide and iron: (Treatment A) the wetted graphite was separated after the mixture of *tert*-butyl halide (bromide, iodide, or chloride) and ALG in the benzene solution was stirred at 50°C for 2 h. (Treatment B) The wetted ALG graphite was separated after bromine (2 ml) was added to the ALG graphite (0.2 g) and sealed in a vial for 2 h. (Treatment C) The HPG graphite was mixed with phenol and *tert*-butyl bromide in the presence and absence of iron.

The surface areas of the graphites were measured at 78 K by nitrogen adsorption using a BET apparatus (Omnisorp, 100CX) after evacuation at 473 K and 1 Pa for 2 h. X-ray photoelectron spectroscopy was carried out using a Shimadzu ESCA 3200 photoelectron spectrometer with Mg $K\alpha$ radiation (1253.6 eV, 8 kV, and 30 mA). The sample was mounted on a holder with silver collodion. Argon etching was done for 5 min before the XPS measurement. The atomic ratios of the XPS O 1s/C 1s and Fe 2p/C 1s on graphite were calculated by

$$\text{(peak area)} \times \text{(sensitivity factor for atoms including apparatus factor)}$$

in the spectra of carbon, oxygen, and iron in the graphites fitted into XPS C 1s (282–294 eV (33)), O 1s (528–540 eV), and Fe 2p (707–730 eV, a broad peak at 711.0 eV (Fe_2O_3)), respectively.

RESULTS AND DISCUSSION

Activation of tert-Butyl Bromide on Graphite

The Friedel-Crafts reaction of phenol with *tert*-butyl bromide on ALG is shown in Fig. 1A (Method A). After *tert*-butyl bromide and ALG were added to benzene solvent and stirred for 1 h, phenol was then introduced into the benzene solution. The reaction products were immediately observed after the phenol addition and *p-tert*-butylphenol together with small amounts of *o-tert*-butylphenol and 2,4-di-*tert*-butylphenol. The concentration of *o-tert*-butylphenol reached a maximum at 60 min and then slowly decreased. The formation of 2,4-di-*tert*-butylphenol gradually increased and reached a steady state after 120 min. The yield of the three compounds was 59%. The same trend was observed for KIG and mineral graphite. However, when phenol and ALG were first mixed in benzene for 1 h before addition of the *tert*-butyl bromide, an induction period was observed for the formation of the reaction products in Fig. 1B (Method B). No reaction product was observed for 20 min after the reaction, although the conversion was about 10%. This is probably due to the

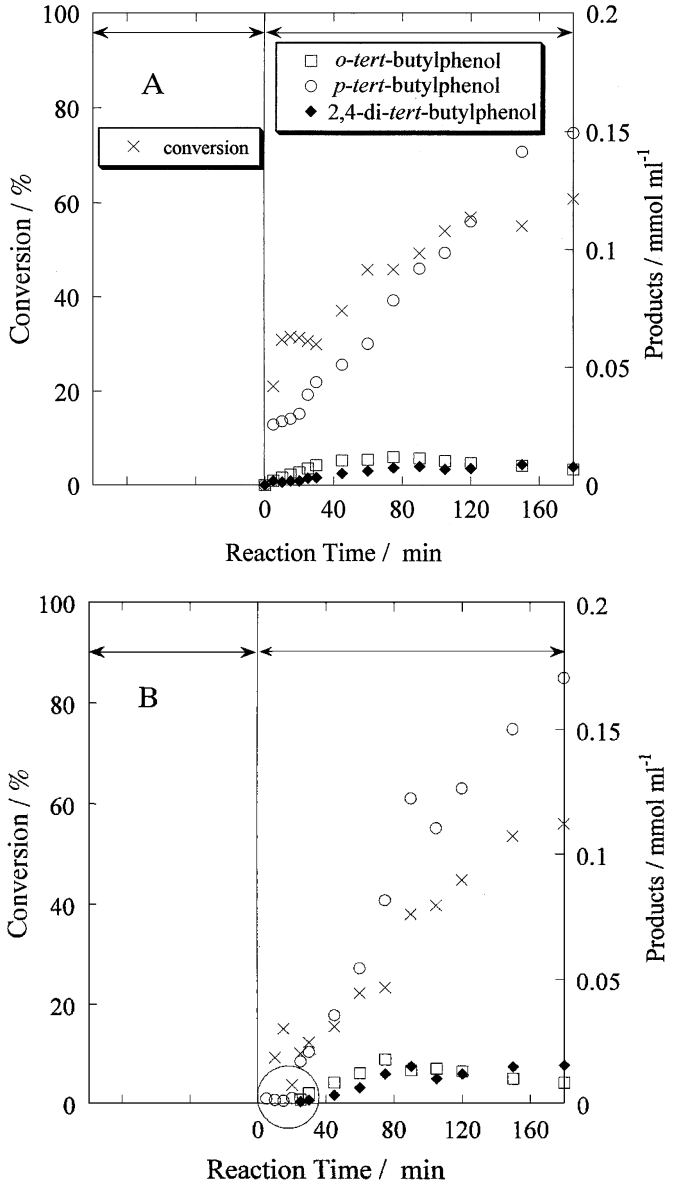

FIG. 1. (A) The addition of phenol after *tert*-butyl bromide and ALG graphite were mixed and stirred in benzene for 1 h. (B) The addition of *tert*-butyl bromide after phenol and ALG graphite were added and stirred in benzene for 1 h.

adsorption of phenol on ALG without the reaction taking place. The reaction products were observed in similar amounts after 20 min. This observation suggested that *tert*-butyl bromide was displaced by some portion of the adsorbed phenol on ALG for some time (induction time) and reacted with the other adsorbed phenol. The induction time was probably the time when *tert*-butyl bromide was adsorbed on the graphite and then activated. Because no induction time was observed on the addition of phenol after mixing with *tert*-butyl bromide and with ALG, the reaction of phenol with *tert*-butyl bromide did not occur until the *tert*-butyl bromide had been adsorbed on the graphite.

Iron-Promoted Graphite

The reaction of phenol with *tert*-butyl bromide in the presence of various graphites is shown in Table 1. The results for the activated charcoal and fullerene are given for comparison. The conversion over ALG was 60% with a 59% yield. The ALG graphite was more reactive with *p-tert*-butylphenol and in a higher yield than $AlCl_3$. The other materials such as activated charcoal and HPG had no yield with small conversion. Fullerene did not exhibit any activity for the reaction. These observations are due to only the physical adsorption of phenol on the surface of graphite without the reaction. Furthermore, the conversion on the graphites and activated charcoal did not depend on the surface area of the samples as shown in Table 1.

The ALG graphite originally contained an amount of iron compared to the other graphites, while no iron was observed in the activated charcoal listed in Table 2. The relationship between the concentration of *p-tert*-butylphenol formed at 4 h and the ratio of iron to carbon (XPS Fe 2p/C 1s atomic ratio) for various graphites is shown in Fig. 2A. The concentration of *p-tert*-butylphenol significantly increased with the increasing Fe 2p/C 1s ratio. The ALG graphite with the Fe 2p/C 1s ratio of 0.012 had a large concentration of *p-tert*-butylphenol. A low concentration of the reaction product was formed for KIG and HPG. No reaction occurred in the presence of activated charcoal with added iron. This result showed that the activity of the graphites was related to the

TABLE 1

Friedel-Crafts Alkylation of Phenol in the Presence of Various Graphites, Fullerene, Activated Charcoal, and $AlCl_3$

Graphite	Surface area ($m^2\ g^{-1}$)	Conversion[a–c] (%)	Yield (%)	Selectivity[d] (%) a	b	c
Synthesis graphite, ALG	11	60	59	3	95	2
Synthesis graphite, KIG	8	40[a]	24	8	85	7
Mineral graphite	1	60[a]	41	9	80	11
Highly pure graphite, HPG	18	22[a]	Trace	—	100	—
Fullerene ($C_{60}+C_{70}$)	0.5	0	0	—	—	—
Activated charcoal	768	50[b]	Trace	—	100	—
$AlCl_3$[e]	—	89[c]	53	2	96	2

[a,b] The difference in conversion and yield was approximately the percentage of the feed amount adsorbed on the [a]graphites (about 20% of phenol) and [b]activated charcoal (50%).

[c] The difference was the percentage of unknown products.

[d] (a) *o-tert*-Butylphenol, (b) *p-tert*-butylphenol, and (c) [c]2,4-di-*tert*-butylphenol were produced in the reaction.

[e] Reaction conditions: phenol (2 mmol), *tert*-butyl bromide (2 mmol), $AlCl_3$ (0.1 g), nitrobenzene (35) (5 ml) at 20°C.

TABLE 2

Contents of Iron and Oxygen in the Graphites and Activated Charcoal from XPS Measurement

Sample	Atomic ratio	
	O 1s/C 1s	Fe 2p/C 1s
Synthetic graphite (ALG)	0.150	0.0117
Synthetic graphite (KIG)	0.036	0.0010
Mineral graphite	0.181	0.0022
Highly pure graphite (HPG)	0.203	0.0009
Activated charcoal	0.435	0

iron content. In order to determine the promoting effect of iron oxide (and chloride) on the reaction of phenol with *tert*-butyl bromide, the addition of Fe_2O_3 to the solution in the presence of HPG is shown in Fig. 2B. The conversion increased with increasing Fe_2O_3 addition. A small amount of Fe_2O_3 (0.008 g) increased the *p-tert*-butylphenol concentration by twice that in the absence of Fe_2O_3. The addition of Fe_2O_3 tremendously shortened the induction time. The reaction occurred on graphite in the presence of both Fe_2O_3 and *tert*-butyl bromide. Furthermore, the addition of $FeCl_3$ to the reaction for HPG exhibited a conversion of 50% at 10 h, and the conversion was similar to that in the presence of Fe_2O_3. The two compounds exhibited the same promoting effect on the reaction of phenol. In the presence of Fe_2O_3, *tert*-butyl bromide was dissociated on graphite to form *tert*-butyl and bromine ions. The latter ion was likely to be associated with iron probably to form $FeBr_2$ and $FeBr_3$ (17, 24) in the layers of graphite. The *tert*-butyl ion reacted with phenol during the exposure to graphite. Hydrogen bromide formed during the reaction generates a Lewis acid which was inserted into the graphite layers.

Reaction of Phenol with tert-Butyl Halides and Alcohol on Graphites and Aluminum Halides

The reaction of phenol with three alkyl halides and *tert*-butyl alcohol in the presence of ALG is shown in Table 3. Aluminum halides were also used in the reaction of phenol instead of ALG for comparison. For the reaction with *tert*-butyl iodide, the conversion was 80% at 4 h with the selectivity of *p-tert*-butylphenol at 64%. The reaction reached a steady state 7 h after the reaction started. For *tert*-butyl bromide, the conversion was 60% at 4 h. However, in the case of *tert*-butyl chloride, the reaction products appeared after 6 h and the conversion at 12 h was 64%. These results showed that *tert*-butyl iodide was the most active of the three halides with a good selectivity of *p-tert*-butylphenol. *tert*-Butyl bromide as the reactant had a good yield but the chloride was the worst. On the contrary, very little reaction took place with *tert*-butyl alcohol. For the mixture of *tert*-butyl bromide (4 mmol) and *tert*-butyl alcohol (4 mmol), the conversion was 57% at 10 h (recovery of 43%) with a selectivity of 45% for *p-tert*-butylphenol, although the conversion was 15% without any yield at 4 h. The conversion of 57% corresponded to the consumed amount of 4.4 mmol for the *tert*-butyl reagents. This value suggested that this amount (0.4 mmol) of *tert*-butyl alcohol did react during the reaction. Note that all the reactions with *tert*-butyl alcohol did not occur on the graphite. On the other hand, the reactivity of the *tert*-butyl halides toward phenol in the presence of $AlCl_3$ decreased in the following order: *tert*-butyl chloride, *tert*-butyl bromide, and *tert*-butyl iodide. This reactivity order of the *tert*-butyl halides in the presence of $AlCl_3$ is different from that in the presence of ALG.

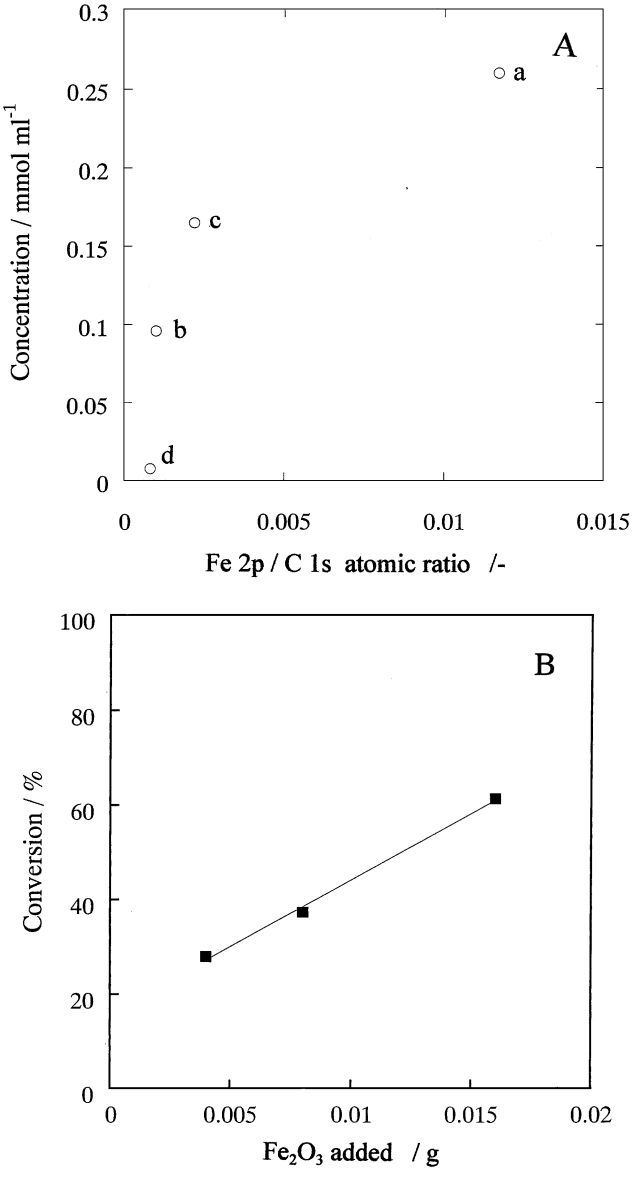

FIG. 2. (A) Relationship between the XPS Fe/C ratio of the various graphites and the concentration of reaction products for 4 h run. (a) ALG, (b) KIG, (c) mineral graphite, and (d) HPG. (B) The addition of Fe_2O_3 to HPG in the reaction of phenol.

TABLE 3

Friedel-Crafts Alkylation of Phenol with Various *tert*-Butyl Halides and Alcohol

Catalyst	*tert*-Butyl halides and alcohol	Time (h)	Conversion[a–c] (%)	Yield (%)	Selectivity[d] (%) a	b	c
Graphite[e]	Cl	12	64[a]	41	16	61	23
	Br	4	60	59	3	94	2
	I	4	80[b]	46	11	64	25
	OH	4	15[a]	0	—	—	—
$AlCl_3$[f]	Cl	1	99[c]	65	1	95	4
	Br	1	89[c]	53	2	96	2
	I	1	77[c]	33	8	75	17

[a,b] The difference in conversion and yield was approximately 20% of phenol adsorbed on the graphites. For [b] *tert*-butyl iodide, about 15% of the feed amount was converted to unknown products.

[c] The difference was the percentage of unknown products.

[d] (a) *o-tert*-Butylphenol, (b) *p-tert*-butylphenol, and (c) 2,4-di-*tert*-butylphenol were produced in the reaction.

[e] Reaction conditions: phenol (8 mmol), *tert*-butyl halide (8 mmol), ALG graphite (4 g), and benzene (20 ml) at 50°C.

[f] Reaction conditions: phenol (2 mmol), *tert*-butyl halide (2 mmol), $AlCl_3$ (0.1 g), nitrobenzene (35) (5 ml), and benzene (20 ml) at 20°C.

Reaction of o-tert-Butylphenol

The reaction of *o-tert*-butylphenol with *tert*-butyl bromide in the presence of ALG is shown in Fig. 3. Although the reaction of *o-tert*-butylphenol did not occur in the absence of *tert*-butyl bromide, 2,4-di-*tert*-butylphenol was formed after the *tert*-butyl bromide addition. Furthermore, *p-tert*-butylphenol and phenol were observed 90 min after the addition. Because this reaction with *tert*-butyl bromide did not take place in the absence of ALG, *tert*-butyl bromide was dissociated to yield *tert*-butyl and bromine ions on graphite. *o-tert*-Butylphenol reacted with the *tert*-butyl ion to yield 2,4-di-*tert*-butylphenol. Also, *o-tert*-butylphenol was isomerized to *p-tert*-butylphenol and dealkylated to phenol with low selectivities. Therefore, the conversion reaction of phenol into *o*- and *p-tert*-butylphenol with *tert*-butyl bromide and the alkylation of *o,p-tert*-butylphenol to 2,4-di-*tert*-butylphenol were reversible.

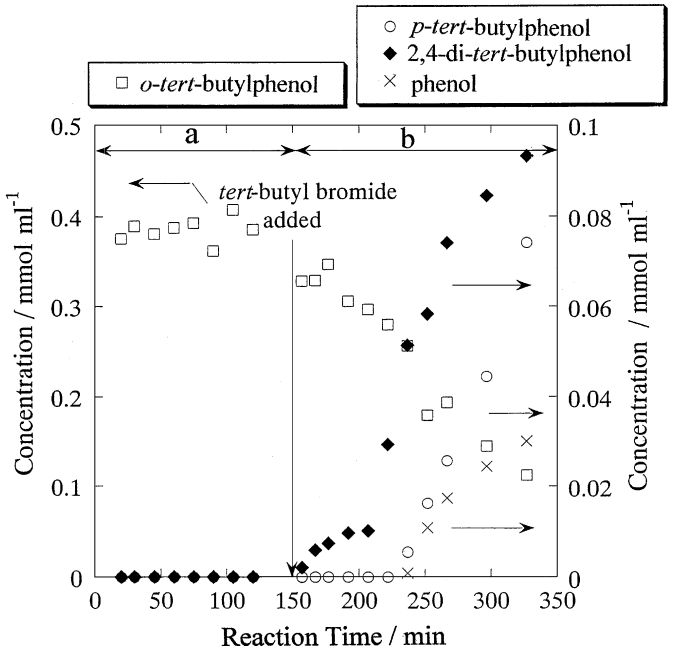

FIG. 3. Change in reaction products with reaction time during the alkylation of *o-tert*-butylphenol at 50°C. (a) *o-tert*-Butylphenol and ALG graphite in benzene. (b) *o-tert*-Butylphenol, *o-tert*-butyl bromide, and ALG graphite in benzene.

Reactivity of Iron-Containing Graphite and $AlCl_3$

The *tert*-butyl iodide and bromide were very reactive with phenol in the presence of ALG and the reaction reached a steady state at 4 h. However, *tert*-butyl chloride was less active and the reaction products were less after more than a 6-h reaction. An induction time was required to form *p-tert*-butylphenol after the addition of phenol (Method A). The formation of *p-tert*-butylphenol in the reaction of phenol with *tert*-butyl halide decreased with the decreasing bond dissociation energy (C–Cl, 330; C–Br, 263; C–I, 209 kJ mol^{-1}) (34). *tert*-Butyl iodide with the smallest bond dissociation energy was then the most reactive toward phenol on ALG. $FeCl_3$ can also insert into graphite (17, 18, 20–22, 29) but *tert*-butyl chloride was much less active in the Friedel-Crafts reaction of phenol. *tert*-Butyl bromide was first dissociated to form *tert*-butyl and bromine ions on graphite. The *tert*-butyl ion reacted with phenol while the bromine ion was associated with the iron. The reaction took place in the layers of graphite based on the carbocation mechanism as follows.

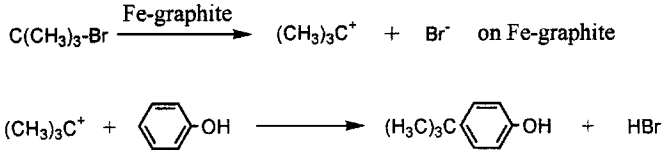

On the other hand, the reactivity of the *tert*-butyl halides in the presence of $AlCl_3$ decreased in the order: chloride > bromide > iodide. The mechanism for the Friedel-Crafts with $AlCl_3$ is well known and fully established. This order of reactivity corresponded to the electronegativity of the halogen (Cl, 3.16; Br, 2.96; I, 2.66). The carbon and halogen atoms of the *tert*-butyl halides were distorted and charged as δ^+ and δ^-; respectively. Therefore, the negative charge was dislocated on the halogen (X) and decreased as follows: chlorine > bromine > iodine. *tert*-Butyl chloride was the most reactive with $AlCl_3$ to form a complex ($AlCl_3X^-$–R^+) that acted as an electron acceptor. This reaction was favorable for producing *p-tert*-butylphenol, because the

tert-butyl halides have larger distorted charges and were coordinated to form a complex with $AlCl_3$. When *tert*-butylalcohol was used as the *tert*-butyl agent, it was hard to react on ALG, because graphite probably showed no Brønsted acid characteristics. However, because the reaction took place with *tert*-butyl bromide in the mixture of *tert*-butyl bromide and *tert*-butyl alcohol, the hydrogen bromide that formed during the reaction reacted with *tert*-butyl alcohol to form the *tert*-butyl carbocation. The *tert*-butyl ion was finally reacted with phenol to form *tert*-butyl phenol in the mixture of the alkyl halide and *tert*-butyl alcohol on graphite.

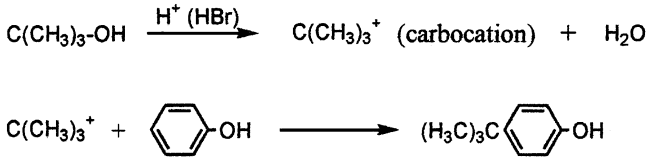

Stage Structure of Graphites and Friedel-Crafts Mechanism

The graphites layered with bromine and iron bromide are reported to be in a second stage structure (16, 17, 19, 20, 22–24). A model of the stage structure of bromine ion insertion is shown in Fig. 4. The distance (d_0) between the graphite layers is 3.35 Å before the reaction. The relationship between the stage structure and the layer distance is as follows:

$$I_c = d_1 + (n - 1) \times d_0, \qquad [1]$$

where I_c is the distance in the stage cycle, d_1 is the layer distance of the graphite between the layers containing compounds, and n is the stage number. The XRD patterns of the ALG treated under the various conditions and the treated HPG are shown in Table 4 and Fig. 5. The peak at $d_1 =$ 11.9 Å ($2\theta = 7.40°$) was observed together with the characteristic peaks for the ALG after the reaction (Fig. 5b) and the HPG treated with Fe_2O_3 and *tert*-butyl bromide (Treatment C). The peak was observed for the wet ALG but disappeared for the dry ALG. No peaks appeared with *tert*-butyl chloride. The untreated ALG showed no enlargement of the layer distance and exhibited a strong peak at $2\theta = 26.48°$ ($d_0 = 3.35$ Å; see d_0 in Eq. [1]) together with small peaks of $2\theta = 42.4$ (100), 44.50 (101), 54.56 (004), and 77.50° (110) as shown in Fig. 5a. The distance (d_1) between the layers increased to 6.98 Å after insertion of the bromine ion into the layers (Treatment B). Bromine ion was inserted into the layered carbons in the stage structures. d_1=7.02 ($2\theta = 12.6°$ and 6.98 Å ($2\theta = 12.7°$) were observed for the ALG treated with *tert*-butyl bromide (Treatment A) (Fig. 5c) and for the ALG treated with bromine (Treatment B), respectively. These values of 7.02 and 6.98 Å were close to d_1 (7.04 Å) of the bromine inserted in the graphite in the

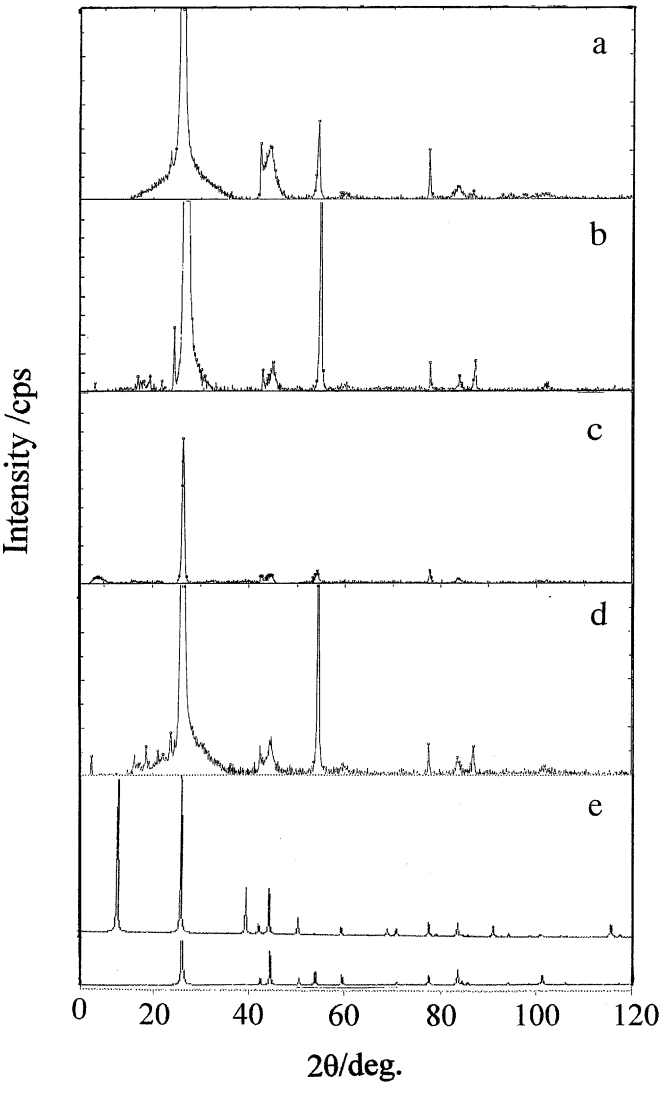

FIG. 5. XRD patterns of active charcoal and the graphites samples after the reaction and under various treatment conditions. (a) ALG graphite before reaction, (b) ALG graphite after reaction, (c) ALG graphite treated with *tert*-butyl bromide, (d) HPG graphite treated with *tert*-butyl bromide and Fe_2O_3, and (e) (lower) XRD spectrum of graphite (lattice constant, $d = 3.35$ Å) and (upper) the layer-inserted graphite ($d = 4.10$ Å) simulated using Cerius2.

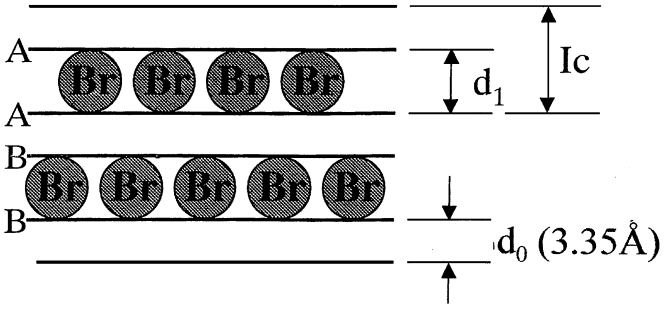

FIG. 4. Stage structure of graphite intercalation with bromine.

TABLE 4

XRD Results of Iron-Containing Graphite Samples after the Reaction and under Various Treatment Conditions

		Treatment (A)[a,c]				
	After reaction[a,b]	*tert*-Butyl bromide	*tert*-Butyl iodine	*tert*-Butyl chloride	Treatment (B)[a,d] Bromine	Treatment (C)[e,f] Fe_2O_3, tert-Butyl bromide
Inserted layer d_1/Å	11.9	7.02	9.46	—	6.98	11.7[e] (11.9)[f]
Graphite phase(002) d_3/Å	3.35	3.35	3.35	3.36	3.36	3.36 (3.35)
I_c/Å	15.25	10.37	12.81	—	10.25	15.06 (15.25)

[a] Before reaction: ALG, phase (002); ASTM card, $2\theta = 26.48^\circ$, $d = 3.35$ Å.
[b] Phenol, *tert*-butyl halide, benzene, and ALG at 50°C for 2 h. $d_1 = 11.9$ Å ($2\theta = 7.40^\circ$).
[c] *tert*-Butyl halide, benzene, and ALG at 50°C for 2 h.
[d] ALG in bromine solution in a vial for 2 h.
[e,f] Phenol, *tert*-butyl bromide, benzene, HPG, and 0.008 g Fe_2O_3 at 50°C for 2[e](5)[f] h. HPG alone (002): $d_0 = 3.35$ Å; no change in graphite distance was observed in the absence of Fe_2O_3 or *tert*-butyl bromide.

literature (18, 22, 23). No peak at $2\theta = 7.40^\circ$ was observed for the HPG with *tert*-butyl bromide in the absence of iron, but the peak was obtained for the treated HPG for 2 and 5 h (Treatment C) (Fig. 5d). The presence of both *tert*-butyl bromide and iron increased the distance between the layers of HPG but not in the presence of either the iron or the *tert*-butyl bromide. Because ALG was likely to contain iron as Fe_2O_3 but not as $FeBr_3$ (Br was not detected by XPS), the Fe_2O_3 was converted to $FeBr_3$ in the presence of hydrogen bromide formed in the reaction of phenol with *tert*-butyl ion. Furthermore, a new peak at $2\theta = 13.0^\circ$ appeared when the distance of the carbon layer increased from 3.35 to 4.10 Å (only two carbon layers), according to the Cerius2 program (Fig. 5e). From the results, the appearance of the peak at $d_1 = 11.9$ Å was due to the wet ALG containing *tert*-butyl, bromine ions, iron, phenol, and benzene. *tert*-Butyl halide was first adsorbed and dissociated to *tert*-butyl and halogen ions on the graphite. The dissociated *tert*-butyl ion entered into the layers of graphite in the presence of iron. The increased layers ($d_1 = 11.9$ Å) are due to the reaction of phenol with *tert*-butyl ion in the presence of iron in the layers similar to the insertion of biphenyl and tetrahydrofuran with potassium in the graphite layer (25). Thus, the peak at $d_1 = 11.9$ Å is due to the reaction of phenol with *tert*-butyl ion which was inserted with iron into the layer of graphite. Another possibility would be that the bromine ion entered the layers of graphite, because d_1 (11.9 Å) in this reaction is approximately 9.9 Å ($FeBr_2$; 9.55 Å for $FeBr_3$ (17, 24)). The layered compound was formed in the two-stage structure. In addition, a new peak was not observed in the presence of *tert*-butyl chloride but formed in the presence of *tert*-butyl iodide, and the graphite assumed the second stage structure ($d_1 = 9.46$ Å). Also, it is reasonable that the d_1 value of *tert*-butyl iodide was greater than that of *tert*-butyl bromide because of the larger iodine ion. Furthermore, activated charcoal exhibited no peaks except for the broad peaks at 2θ equal to about 20°, even in the presence of iron. The activated charcoal contained several kinds of carbonaceous carbon species and oxygen-containing groups such as hydroxyl, carbonyl, and carboxyl groups (33). The activated charcoal was not active in the Friedel-Crafts reaction; therefore, these functional groups did not affect the reaction, but the rich π-electron carbons of the graphite were responsible for the adsorption and dissociation of the *tert*-butyl halide on graphite and the reaction with phenol.

The mechanism for the Friedel-Crafts reaction of phenol with *tert*-butyl bromide on graphite proceeded in several steps as shown in Fig. 6. *tert*-Butyl bromide was first adsorbed on graphite and dissociated to *tert*-butyl and

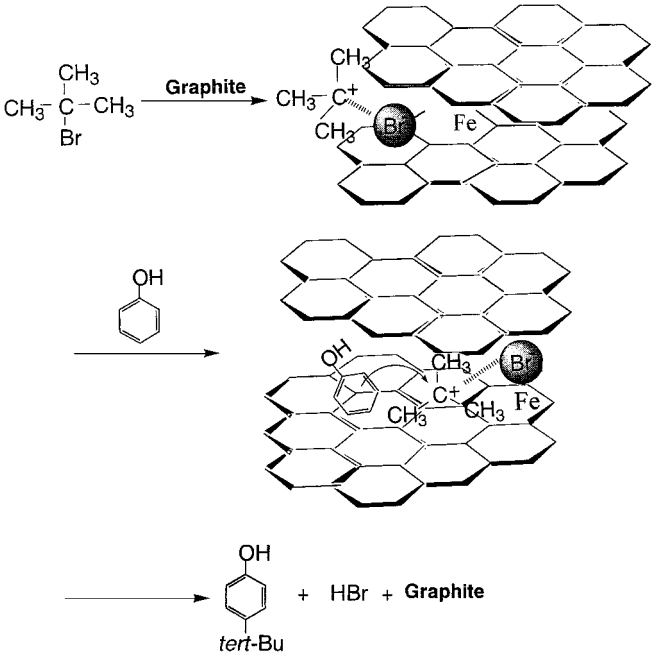

FIG. 6. Reaction mechanism for the Friedel-Crafts of phenol with *tert*-butyl bromide in the presence of iron-containing graphite.

bromine ions during the initial stage of the reaction. Fe_2O_3 or iron bromide (formed with hydrogen bromide) assisted the removal of a bromine ion from *tert*-butyl bromide (probably as a complex of the iron bromide) in the layers of graphite. The *tert*-butyl ions were inserted into the layers of graphite and reacted at the *para* position of the phenol to yield *p-tert*-butylphenol, while the bromine ion reacted with the hydrogen of *tert*-butylphenol to yield hydrogen bromide in the graphite.

CONCLUSIONS

The Friedel-Crafts reaction of phenol with *tert*-butyl halides on graphite decreased in the following order: iodide, bromide, and chloride. *tert*-Butyl iodide was the most active in the Friedel-Crafts of phenol in the presence of graphite, whereas it was the least reactive in the presence of $AlCl_3$. Aluminum chloride was very highly active in phenol, while graphite was mildly reactive in phenol. The reaction did not occur until after the induction time when *tert*-butyl bromide was adsorbed and dissociated into *tert*-butyl and bromine ions on graphite. Bromide and iodide were readily inserted into the layered carbons of graphite, while chlorine was inserted with difficulty, and therefore hardly reacted with phenol. Fe_2O_3 or iron bromide formed during the reaction promoted the removal of bromine ion from *tert*-butyl bromide and the insertion of *tert*-butyl ion into the layers of the graphite. Phenol with *tert*-butyl ion in the presence of iron entered the layers of graphite in the two-stage structures. The Friedel-Crafts alkylation of phenol on graphite is accompanied by isomerization and dealkylation.

REFERENCES

1. Armengol, E., Corma, A., García, H., and Primo, J., *Appl. Catal. A* **149**, 411 (1997).
2. Miller, J. M., Goodchild, M., Lakshmi, J. L., Wails, D., and Hartman, J. S., *Catal. Lett.* **63**, 199 (1999).
3. Wu, X., and Anthony, R. G., *J. Catal.* **252**, 112 (1999).
4. Choudhary, V. R., Jana, S. K., and Kiran, B. P., *Catal. Lett.* **59**, 217 (1999).
5. Jun, S., and Ryoo, R., *J. Catal.* **195**, 237 (2000).
6. Kamitori, Y., Hojo, M., Matsuda, R., Izumi, T., and Tsukamoto, S., *J. Org. Chem.* **49**, 4165 (1984).
7. Izumi, Y., Onaka, M., and Urabe, K., *Appl. Catal. A* **132**, 127 (1995).
8. Quaschning, V., Deutsch, J., Druska, P., Niclas, H.-J., and Kemnitz, E., *J. Catal.* **177**, 164 (1998).
9. Heidekum, A., Hamm, M. A., and Hoelderich, F., *J. Catal.* **188**, 230 (1999).
10. Reddy, P. R., Subrahmanyam, M., and Kumari, V. D., *Catal. Lett.* **61**, 207 (1999).
11. Wang, Q. L., Ma, Y., Ji, X., Yan, H., and Qiu, Q., *J. Chem. Soc., Chem. Commun.* 2307 (1995).
12. Cativiela, C., Garcia, J. I., Garcia-Matres, M., Mayoral, J. A., Figueras, F., Fraile, J. M., Cseri, T., and Chiche, B., *Appl. Catal. A* **123**, 273 (1995).
13. Clark, J. H., Kybett, A. P., Macquarrie, D. J., Barlow, J., and Landon, P., *J. Chem. Soc., Chem. Commun.*, 1353 (1989).
14. Laszlo, P., and Mathy, A., *Helv. Chim. Acta* **70**, 577 (1987).
15. (a) Izumi, Y., Urabe, K., and Onaka, M., *Catal. Surveys from Jpn.* **1**, 17 (1997); (b) Urabe, K., Hisada, M., and Izumi, Y., Abstracts, 7th Int. Symp. on Relation between Homogeneous and Heterogeneous Catalysis, Tokyo, p. 437, 1992.
16. Kagan, H. B., *Chemtech* 510 (1976).
17. Stumpp, E., *Mater. Sci. Eng.* **31**, 53 (1977).
18. Herein, D., Braun, T., and Schlögl, R., *Carbon* **35**, 17 (1997).
19. Mordkovich, V. Z., *Synthetic Metals* **63**, 1 (1994).
20. Dresselhaus, M. S., and Dresselhaus, G., *Adv. Phys.* **30**, 139 (1981).
21. Inagaki, M., and Ohira, M., *Carbon* **31**, 777 (1993).
22. Takahashi, Y., *in* "New Development of Applied Carbon Material Technology" (Japanese) (M. Inagaki, Ed.), pp. 93–115. Jisk., Tokyo, 1988.
23. Sasa, T., Takahashi, Y., and Mukaibo, T., *Carbon* **9**, 407 (1971).
24. Stahl, V. H., *Z. Anorg. Allg. Chem.* **428**, 269 (1977).
25. Beguin, F., Setton, R., Hamwi, A., and Touzain, P., *Mater. Sci. Eng.* **40**, 167 (1979).
26. Herein, D., Braun, T., and Schlögl, R., *Mol. Cryst. Liq. Cryst.* **245**, 189 (1994).
27. Kodomari, M., Suzuki, Y., and Yoshida, K., *J. Chem. Soc., Chem. Commun.* **1569**, 1957 (1997).
28. Suzuki, Y., Kodomari, M., and Matushima, M., *Chem. Lett.*, 319 (1998).
29. Göndös, G., and Kapocsi, I., *J. Phys. Chem. Solid* **57**, 855 (1996).
30. Lalancette, J.-M., Fournier, M.-J., and Thiffault, R., *Can. J. Chem.* **52**, 589 (1974).
31. Tsuchiya, S., Fujii, K., Mitsuno, T., Sakata, Y., and Imamura, H., *Bull. Chem. Soc. Jpn.* **64**, 1011 (1991).
32. Rashkov, I., Panayotov, I., and Gitsov, I., *Poly. Bull.* **4**, 97 (1981).
33. Wild, U., Pfänder, N., and Schlögl, R., *Fresenius,' J. Anal. Chem.* **357**, 420 (1997).
34. McMurry, J., "Organic Chemistry," 5th ed. Brooks/Cole, CA, 2000.
35. Pivsa-Art, S., Okuro, K., Miura, M., Murata, S., and Nomura, M., *J. Chem. Soc., Perkin. Trans. I*, 1703 (1994).